2017

An Analysis of Stimuli Responsive Biomaterials using Raman Spectroscopy and Computational Studies

Gretchen Harknett
University of Mississippi. Sally McDonnell Barksdale Honors College

An Analysis of Stimuli Responsive Biomaterials using Raman Spectroscopy and Computational Studies

By: Gretchen Laurel Harknett

A thesis submitted to the faculty of the University of Mississippi in partial fulfillment of the requirements of the Sally McDonnell Barksdale Honors College.

Oxford
May 2017

Approved by:

_____
Advisor: Professor Nathan Hammer

_____
Reader: Professor Davita Watkins

_____
Reader: Dean Sullivan-González

ACKNOWLEDGEMENTS

I would like to thank my family for their tremendous support throughout my academic career here at the University of Mississippi. This journey would not have been possible without them. I would like to thank my research advisor, Dr. Nathan Hammer, for pushing me and helping me excel academically and for allowing me to work in his research lab. Thank you for believing in me. I would also like to give a special thanks to Louis McNamara for helping me every step of the way and being patient with me. You were the best mentor I could've asked for. I would like to thank Davita Watkins for allowing me to join in on her studies and guiding me along the way.

ABSTRACT

This thesis involves the computational and spectroscopic exploration of the linear dendritic block copolymer, poly(L-lactide)-poly(amido-amine), (PLA-PAMAM), under different environmental conditions using Raman spectroscopy, in hopes to utilize it in future effective and cost-efficient drug delivery systems. Janus dendrimers, a material made up of two different dendrimer portions, are currently being studied in great detail, as they possess many attractive features for materials scientists looking to develop ways for drugs to be delivered in more efficient manners than currently available to physicians. The instrumentation used to conduct this thesis is a high resolution Raman spectrometer. Computationally, *Gaussian 09* was employed to model PLA-PAMAM, and to compare and explain the experimental data. Raman spectroscopic data was also taken on PAMAM-boc, which is the hydrophilic portion of the PLA-PAMAM structure. Spectra were recorded on the neat molecules alone, surrounded by a drop of water, aggregated in water, and aggregated in a pH solution of 9.6. Because of the potential use of PLA-PAMAM as a drug delivery system in the body, understanding the effects of its interactions with water and similar environments with an acidic or basic pH is important to development of effective drug delivery systems. A pH of 9.6 was chosen because delivery methods through the eyes are a potential mode of entry, and the eyes are more basic than a normal pH of 7. The results and discussion found in this thesis help elucidate shifts in vibrational spectra as PAMAM-boc and PLA-PAMAM are placed in different environments, specifically water and a pH solution of 9.6.

TABLE OF CONTENTS

Title Page 1
Copyright Page 2
Acknowledgements 3
Abstract 4

1 Introduction 6
1.1 Biomaterials 6
1.2 Smart Polymers 6
1.3 Hydrogels and Tissue Scaffolds 8
1.4 Dendrimers and Dendrimer-Based Derivatives 10
1.5 PLA-PAMAM 13

2 Spectroscopy 16
2.1 Definition 16
2.2 Electromagnetic Radiation 16
2.3 Vibrational Spectroscopy 20

3 Raman Spectroscopy 24
3.1 Instrumental Design 24
3.2 Raman Spectroscopy Principles 25
3.3 Computational methods 29

4 Raman Spectroscopic Results of PLA-PAMAM 31
4.1 Experimental Results and Data Analysis 31
4.2 Theoretical Results and Data Analysis 39
4.3 Discussion and Conclusions 42

References 45

Chapter 1: Introduction

1.1 Biomaterials

Biomaterials, specifically stimuli responsive biomaterials, and the way they interact in the body is an up and coming topic that has many people interested and excited. With investigation and experimentation, the advancements in this area could bring about massive changes in the medical world and enhance the way medicine is used. Biomaterials are non-viable materials that can be constructed in a lab, incorporated into the body, and exist in the body's natural environment. They serve many purposes, including forming synthetic organs or replenishing or taking the place of bone or tissue. "A wide variety of polymers are used in medicine as biomaterials. Their applications range from facial prostheses to tracheal tubes, from kidney and liver parts to heart components, and from dentures to hip and knee joints". [1]

1.2 Smart Polymers

Biomaterials that respond to different stimuli – light, pH, or temperature for example – are being utilized in order to promote a more direct and controlled way of delivering drugs that are in a biologically active form. One of the problems of current drug delivery methods is that the drug levels spike immediately after injection and then drastically decrease again. These drug delivery systems using stimuli responsive biomaterials will allow for a more controlled, meticulous way of delivering these drugs in a biologically active state when the body is in need of them and stops the release of the drug when it is no longer needed.[2] The biomaterials will degrade at a slower, more

controlled rate that allows the body to avoid the single initial spike in drug concentration. The researchers that are developing and studying these stimuli responsive biomaterials call them "smart polymers".[3] They form an intelligent drug delivery system that allows chemicals to be released at a specific time and place when a distinctive stimulus for that stimuli responsive biomaterial is present. Depending on the particular stimuli present, different responses are elicited that cause the release of the drug. For instance, in the case of a pH stimulus, the smart polymer could change its overall conformation. The pH-sensitive polymer will gain or release a proton based on its acidity or basicity, and this rapid change in net charge of the polymeric chain causes the polymer to release the drug.[3] In the case of temperature sensitive stimuli, the polymer's solubility is what changes in order to release the drug. Bioresponsive polymers are specific smart polymers that respond to the stimulus of natural occurring chemicals and molecules that are found in the physiological environment of the body. These specific smart polymers possess certain functional groups that are able to interact with natural molecules in the body, like glucose or an antigen.[3] "An on-off regulation for insulin release is effective in response to external glucose concentration by utilizing the reversible complex formation between glucose and the phenylboronic acid group. The gels operate at physiological pH bearing phenylborate derivatives as a glucose-sensing moiety".[2] In this case it is hydrogels that are being utilized for the drug delivery, but the concept is the same for smart polymers.

1.3 Hydrogels and Tissue Scaffolds

Similar to smart polymers, there have also been many specific studies that target the development of particular tissue scaffolds that respond to different stimuli, their purpose being to increase the speed of skin healing by increased cell proliferation, increased cell communication, and increased vascularization. Macropores and macroporosity are a vital component to many of these scaffolds and their ability to regenerate tissue. Macropores are the spacious holes found within the hydrogel tissue scaffolds that allow the influx of materials needed for promoting tissue formation. As shown in Figure 1.3.1, "Macropores within hydrogels are important microstructures that promote tissue formation by facilitating diffusion, cell proliferation, migration, and extracellular matrix (ECM) production".[4]

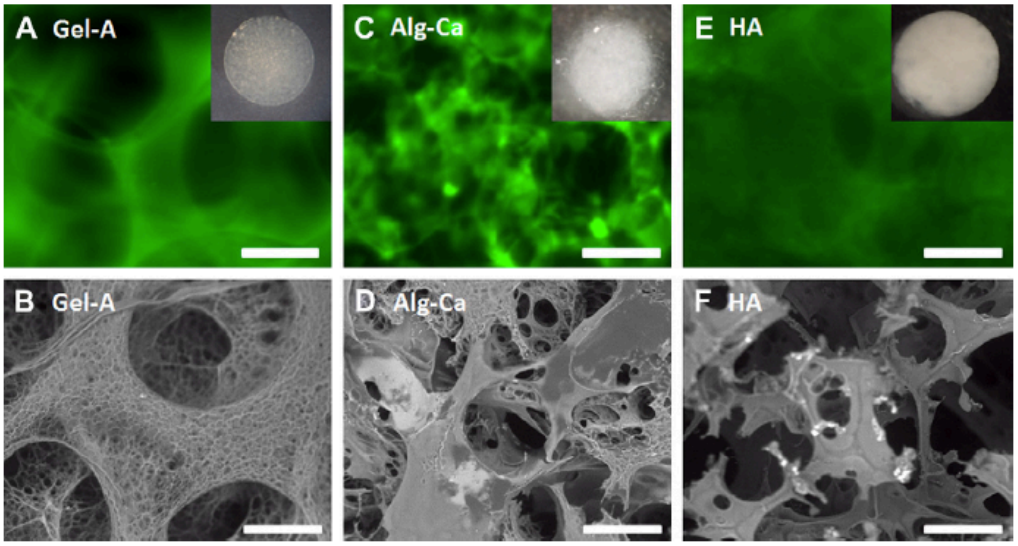

Figure 1.3.1 – Morphology of mono-porogen containing scaffold after porogen removal as shown by fluorescence imaging and scanning electron microscopy. Scaffold morphology after the removal of porogens based on type A gelatin (Gel-A) (A, B); alginate-calcium (Alg-Ca) (C, D) and hyaluronic acid (HA) (E, F).[4]

The ability to dynamically tune their size and density is crucial for this tissue regeneration within these tissue scaffolds. After exposure to specific stimuli at several points in time, macropores formed a highly interconnected network within the 3D hydrogels and the stimuli responsive porogens that make up the hydrogels can serve as cell-delivery vehicles for temporal cell release within the 3D scaffolds.[4] The ability to tune this macroporosity and the networks formed within the scaffolds that cause an increase in cell proliferation and survival can facilitate the desired fate of cell and tissue reconstruction.

One of the many issues dealing with tissue reconstruction among wounds is the lack of cell permeation and vascularization. One of the main determinants in the wound healing response is oxygen. In a wound setting, oxygen is reduced to form a reactive oxygen species (ROS), such as a superoxide anion.[5] Superoxide anions promote phagocytic cells to fight infection and also drive endothelial cell signaling such as required during angiogenesis.[5] Specific tissue scaffolds that respond to a changing pH are being utilized to generate a pro-healing reaction. The scaffold density fluctuates in response to the pH and the fluctuating density and structure of the scaffold leads to an increase in oxygen and nutrient delivery to the tissue in need. When the pH decreases, the scaffold swells and tissue regeneration processes are activated. "pH responsive scaffolds advanced the formation of granulation tissue *in vivo*. The pro-healing response – an increase in growth factors and cytokines to encourage regeneration over inflammation – was induced by scaffolds that can sense and response mechanically to their environment".[6] Tissue scaffolds are also being functionalized with certain types of

drugs that are implanted or injected into the body. Figure 1.3.2 shows the difference in cell composition of a non pH-responsive scaffold versus a pH-responsive scaffold.

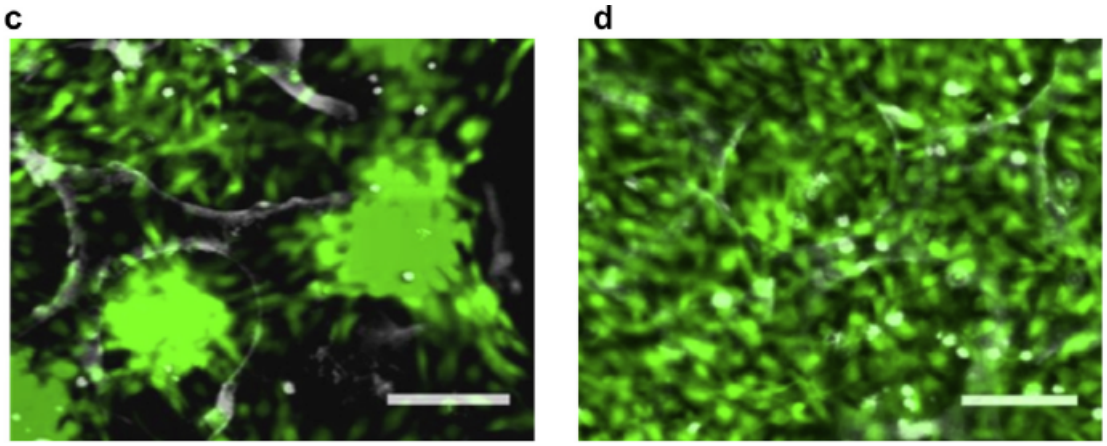

Figure 1.3.2 – Fluorescent micrographs of NIH/3T3 cells seeded on (c) HEMA and (d) pH-sensitive DMAEMA/HEMA scaffolds after 72 h, stained with the Live/Dead assay.[6]

The cells seeded on the HEMA are clumped and unable to grow evenly. On the pH-sensitive DMAEMA/HEMA scaffold, the cells were able to grow homogenously throughout the scaffold.[6]

1.4 Dendrimers and Dendrimer-Based Derivatives

In order to make the delivery of drug more efficient and enhance their biomedical applications, the Watkins group focuses on the development and analysis of dendrimers, specifically Janus dendrimers. Dendrimers are a family of three-dimensional, nanoscale hyperbranched polymers characterized by a unique symmetrical branched architechture.[7] The name dendrimer was derived from the Greek word ‘dendron’ meaning ‘tree,’ which is representative of their distinct ‘tree-like’ branched architechture.[7]

Dendrimers can be synthesized in a convergently or divergently. However, most dendrimers are synthesized using the divergent approach. Thus, dendrimers are grown exponentially from a core molecule and each subsequent radial branch added onto the core is termed as a generation[7] as shown in Figure 1.4.1.

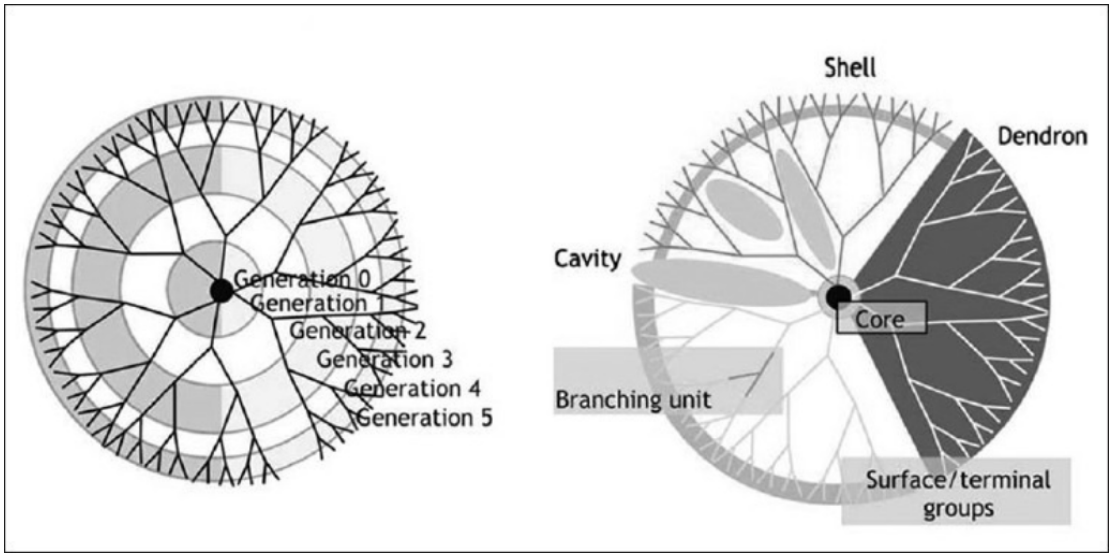

Figure 1.4.1 – Basic Structure of a Janus Dendrimer Aggregate[8]

A dendrimer with a larger number of generations has an equally larger amount of terminal groups. The amount of terminal groups or surface groups plays a significant role in determining their biological interactions and material properties.[9] Chemical modifications to the surface of the dendrimer terminal groups can reduce unwarranted, cytotoxic side effects. For example, PAMAM is a dendrimer whose terminal branches can be decorated with amine groups to direct which interactions will occur and to monitor cytotoxicity.[7] The dendrimers are very small and nanodiverse.

Janus dendrimers and linear-dendritic block copolymers (LDBCs) are dendrimer-based derivatives and they serve many functions, particularly in the development of a controlled drug delivery system. Janus dendrimers are comprised of two or more kinds

of dendritic backbones, usually two segments with different chemical structures.[10] Janus dendrimers have been known to self-assemble into dendrimersomes in aqueous environments, giving them a desirable vesicle-like structure that is perfectly equipped to encapsulate hydrophobic materials.[11] These heterogeneous Janus dendrimers have shown promise in many biomedical applications, including nanocarriers for RNAi therapeutics, transferring genetic material into cells, and a wide variety of other applications.[12 12b]

LDBCs are another dendrimer-based derivative that are comprised of a branched dendrimer as described above and a linear block copolymer. These two materials provide unique structural properties that contribute to their potential drug delivering capabilities. The dendrimer portion of the LDBCs is usually hydrophilic and the linear block copolymer of the LDBCs is usually hydrophobic, making the overall LDBC amphipathic. Like Janus dendrimers, LDBCs also self-assemble into aggregates when they are in aqueous solution and these aggregates are capable of loading hydrophobic drugs into the linear block copolymer region of the LDBCs. The dendrimer region has been reported to enhance the thermodynamic stability of self-assembled micelles and stabilize the complexation between cationic polymers and nucleic acids[7] as shown in Figure 1.4.2.

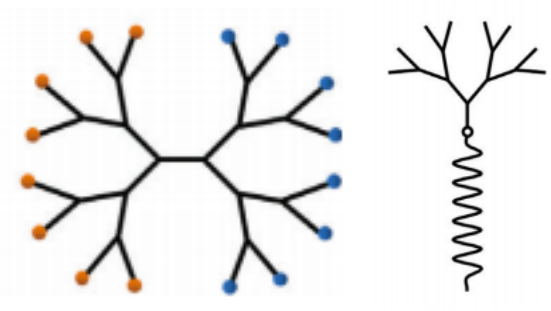

Figure 1.4.2 – Basic structure of Janus dendrimer (left); basic structure of a LDBC(right)[7]

1.5 PLA-PAMAM

In this research and thesis, the dendrimer of choice is poly(L-lactide)-poly(amido-amine), or PLA-PAMAM, which is a linear-dendritic block copolymer. PLA makes up the linear portion of the polymer and PAMAM making up the dendritic branched portion of the polymer. As described above, PLA-PAMAM is safe to use in the body because the surface of the PAMAM, the terminal tips of the branches, is decorated with neutral functional groups that direct non-cytotoxic interactions that occur in the body.[7] Because of the amphipathic nature of PLA-PAMAM, these biomaterials aggregate in water, forming bilayered vesicle like structures. The aggregation in water is random yielding a mixture of nanoparticles. The hydrophilic PAMAM portions form the outer surface of the vesicle and the hydrophobic PLA portions form the inner workings of the vesicle that is perfect for encapsulating drugs. In order for them to function as drug delivery systems, they must be soluble in water so the body can uptake them. PLA-PAMAM is a biodegradable, biocompatible polymer material whose self-assembly and bilayered vesicle like structure will allow for a more controlled, efficient method of delivering drugs into the body. Biocompatibility is a general term referring to the biological properties of the material in terms of toxicity and potential of eliciting an immune response in biological systems.[13] The Janus dendrimers have to be specific because these materials will lose their efficiency if the body attacks them when they are inserted into the body. In order to make these dendrimers more effective, researchers have tried to find a way to make the uptake and releasing of these drug molecules by the dendrimers more efficient.

This research project delves into the fundamentals of PLA-PAMAM and the way the biomaterial behaves when it interacts with water as well as how the biomaterial changes when the pH is altered. Specifically, this research is important because it studies the way these aggregates form, how they uptake drugs, and how they degrade. In addition, current research of LDBCs as potential drug delivery systems (DDS) indicate that the self-assembly behavior is not well understood.[14] Overall, the fundamental findings of this research are going to aid Dr. Watkins in determining the nature of poly(L-lactide)-poly(amido-amine) in the body and its drug delivering capabilities. In order to study the entire PLA-PAMAM structure, part of the material was studied prior to the whole LDBC. PAMAM-boc is the hydrophilic portion of the material, boc ($C_5H_9O_2$) being the outer shell covering the terminal tips of the branches of PAMAM and making it a neutral material. PAMAM without the shell is a charged structure. Molecule structures of PLA-PAMAM and PAMAM-boc are shown in Figure 1.4.3.

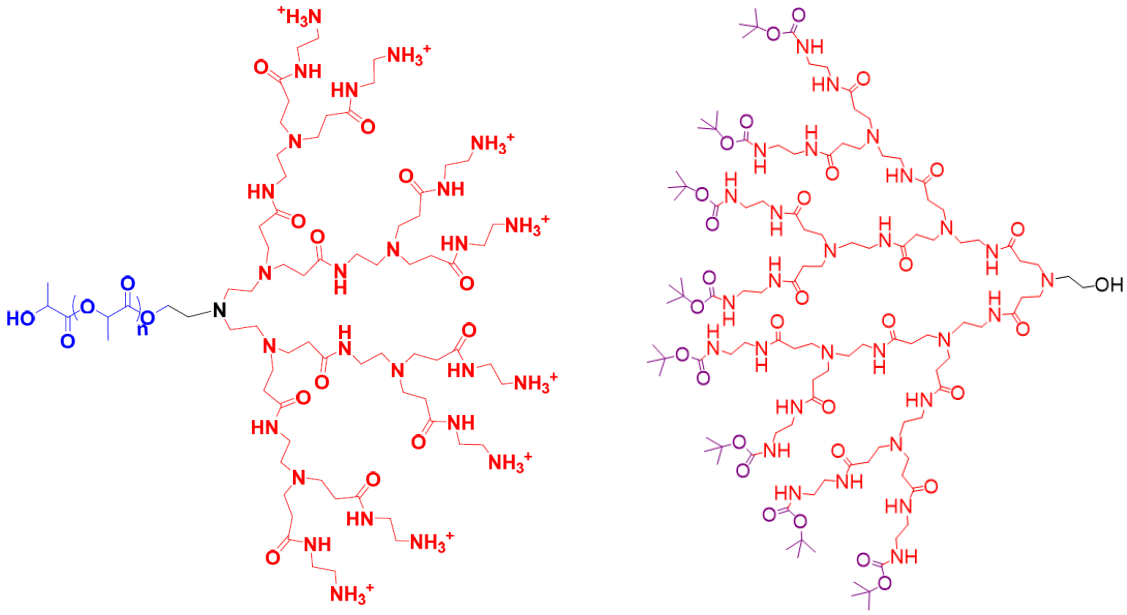

Figure 1.4.3. – PLA-PAMAM structure (left); PAMAM-boc structure (right)

These findings will aid Dr. Watkins in ongoing studies on the polymeric biomaterial and how they can expect the biomaterial to act in the presence of the natural environment aspects of the body.

Chapter 2: Spectroscopy

2.1 Definition

In simple terms, spectroscopy is the study of light interacting with matter. Light interacts with matter in different ways based on the molecular makeup of the sample. Without destroying the sample, this interaction can provide a wide array of important physical and chemical properties of the sample being studied that can be applied to research in various fields, such as biology, forensics, geology, pharmaceutics, and more.[15]

2.2 Electromagnetic Radiation

Electromagnetic radiation is commonly referred to as light and it has many unique characteristics. Notably, it resembles both a wave and a particle, and this is known as its wave-particle duality. In the 1850's Maxwell proved that light acts as a transverse propagating wave with electric and magnetic fields.[16] To this wave like description of the electromagnetic radiation, quantum mechanics adds the concept of particle like description of electromagnetic energy called photons.[17] The photons of light have a given wavelength and frequency, which dictates the energy of the photon. Einstein's equation shows the relationship between these variables, where E is the energy of the light in Joules, h is Planck's constant 6.626×10^{-34} J/s, v is the frequency of the light in Hertz, c is the speed of light 3.00×10^{8} m/s, and λ is the wavelength of light in meters. The following equation shows the duality of light as both a wave with a frequency and wavelength and as a particle with a certain energy.

$$E = h\nu = \frac{hc}{\lambda}$$

The energy of light is directly proportional to the frequency of the light and indirectly proportional to the wavelength of the light. For example, light with a smaller wavelength and higher frequency will have a higher energy than light with a bigger wavelength and a lower frequency. When a particular radiation is characterized by a single frequency, it is said to be monochromatic.[17] A radiation beam of different frequencies is said to be polychromatic.[17]

The electromagnetic spectrum is shown in Figure 2.2.1 and consists of an array of electromagnetic radiation with different vibrational frequencies. The human eye can see a small fraction of the electromagnetic spectrum, seeing electromagnetic radiation with frequencies between 400 and 700 roughly. This is called visible light.

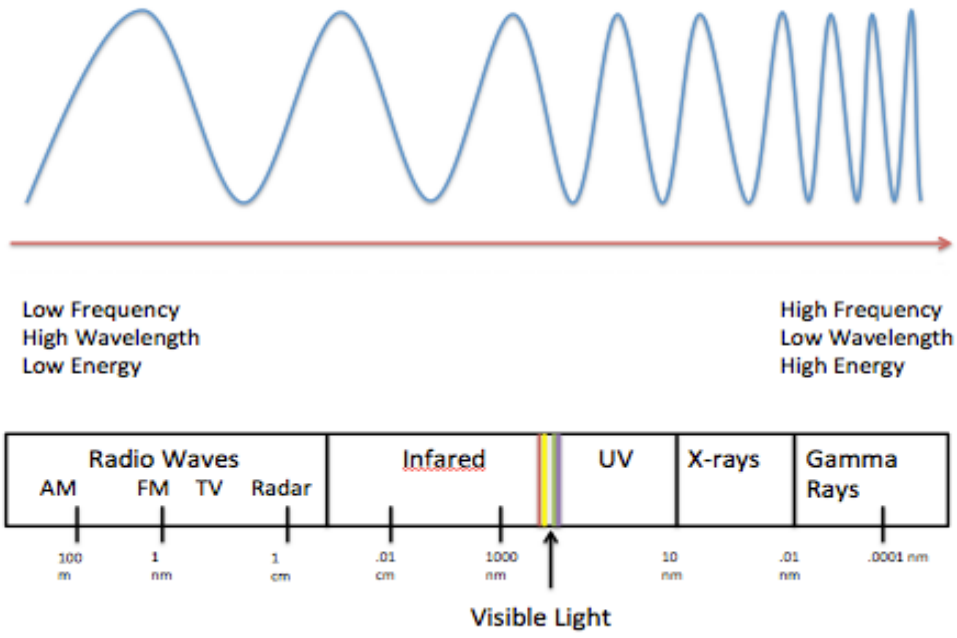

Figure 2.2.1 – The Electromagnetic Spectrum

In order to understand spectroscopy and the way light interacts with matter, it is crucial to have a good understanding of the nature of light and its properties. Electromagnetic radiation consists of photons, which are little bundles of light with specific energies. Photons interacting with the matter cause transitions between energy levels. Photons of light can either be absorbed by the matter, scattered by the matter, or may pass through the matter unaffected at all.[18] There are specific types of spectroscopy that take advantage of absorbance and other types of spectroscopy that study the scattering effect. In absorption spectroscopy, the amount of energy of radiation lost from the incident light is the amount of energy required by the photon to promote the molecule to transition from one energy level to a higher energy level state; the spectrometer measures that change in energy, specifically the loss in energy of radiation from the light.[18]

Molecules absorb photons of light that promote them to a higher energy level state, and this process is accompanied by emission, as shown in Figure 2.2.1.. Emission is the relaxation of molecules from a higher excited energy state to a lower energy state and can occur either spontaneously or stimulated. Spontaneous emission is the random decay from a higher energy state to a lower energy state after a certain amount of time and the released energy is in the form of a photon that is emitted in a random direction.[19] Stimulated emission occurs when the molecule relaxes to a lower energy state caused by an incoming photon. The photon that is released in stimulated emission follows the path of the incident light that initially caused the emission, and the light appears brighter.[19] This concept is the same concept that was used when creating a laser. This understanding

of coherent light sources is important because spectrometers use lasers as their light source.

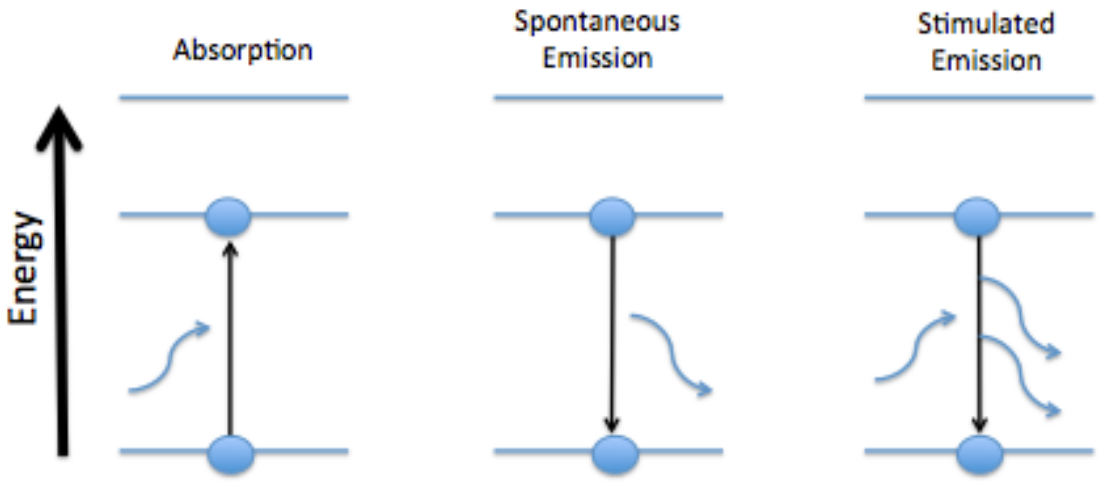

Figure 2.2.1 – Illustration of absorption, spontaneous emission, and stimulated emission

Einstein's coefficients, B_{12}, B_{21}, and A_{21}, are used to describe the processes of absorption, stimulated emission, and spontaneous emission, respectively. These coefficients help determine the rate at which these processes occur. For example, the B coefficients are defined in terms of the transition rates for (induced) absorption W^i_{12} and induced emission W^i_{21}.[20] The following equations are the relative rates of absorption, stimulated emission, and spontaneous emission respectively, where $\rho(v)$ is the energy density per unit angular frequency interval and N is the number of atoms in the level designated by the subscript.[20]

$$W^i_{12} = B_{12}\,\rho(v)\,N_1$$

$$W^i_{21} = B_{21}\,\rho(v)\,N_2$$

$$W^s_{21} = A_{21}\,N_2$$

Because stimulated emission and absorption involve an incident photon of a particular frequency, they are affected by p(v).

When the system is in equilibrium, the rate of absorption is equal to the rate of emission (stimulated and spontaneous). Einstein used this idea to formulate an equation that relates the stimulated emission (B_{21}) to the spontaneous emission (A_{21}), where h is Planck's constant, c is the speed of light, and v is the frequency of light.[21]

$$\frac{A_{21}}{B_{21}} = \frac{16\pi^2 h v^3}{c^3}$$

For a system to have energy removed from it, there must be excited energy in that system to start out with. This means that some excited energy state must be populated initially.[22] The relative populations of the atoms occupying the energy levels are given by the Boltzman distribution equation below:

$$\frac{N_2}{N_1} = \frac{g_2}{g_1} e^{\frac{-hv}{kT}}$$

where hv is the energy difference of the two levels, k is the Boltzman constant that is equal to 1.38 x 10^{-23} J/K, T is the temperature in K, and g_2 and g_1 refer to the relative degeneracies for the energy states. This equation gives the relative ratio of atoms in the excited state to the atoms in the ground state.[21]

2.3 Vibrational Spectroscopy

Vibrational spectroscopy is the study of radiation within the infrared region of the electromagnetic spectrum interacting with the vibrational motions of a molecule. The

vibrational modes of a molecule give rise to the molecular structure with the assistance of vibrational spectroscopy. In infra-red spectroscopy the absorption and emission of radiation is primarily due to changes in the vibrational energy of the system through which the radiation is passing (absorption) or from which it is emanating (emission).[22] Not only does radiation get absorbed or emitted in vibrational spectroscopy, but its also gets scattered. The total energy of a molecule can be represented as a sum of contributions from electronic, vibrational, rotational and translational parts.[23] Each area of the electromagnetic spectrum is associated with a change in energy because of transitions between energy levels based on the wavelength of light. Absorption or emission of quanta in the mid-infrared region of the spectrum and scattering of visible light by vibrational molecules bring about changes of vibrational energy leading to IR and Raman spectra, respectively.[23] Molecular vibrations are explained using the harmonic oscillator and the Schrödinger equation gives rise to the vibrational energy levels of a molecule. Selection rules based on the harmonic oscillator approximation tell which transitions are expected to have zero intensity and which have non-zero intensity.[17] Transitions predicted to have zero intensity are said to be forbidden and those predicted to have non-zero intensity are said to be allowed.[17] Vibrational transitions are illustrated in the potential energy diagram in Figure 2.2.2, and these transitions are what the spectrometer detects.

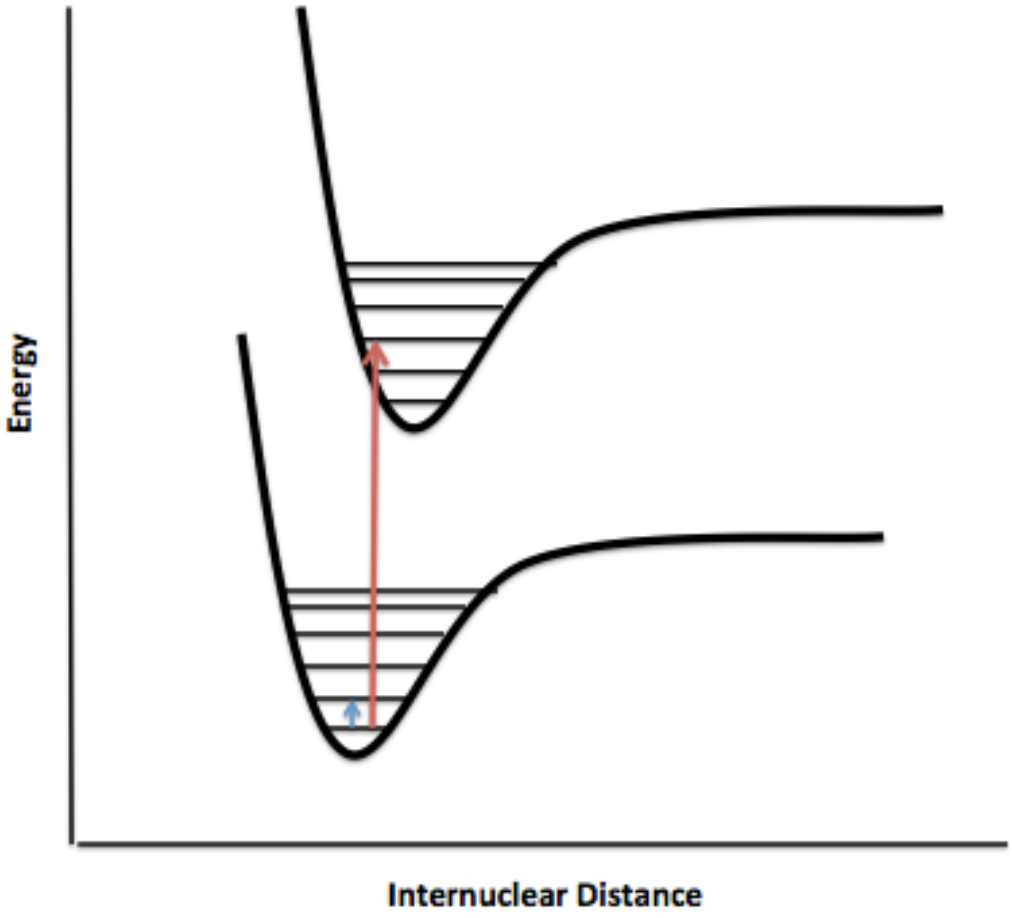

Figure 2.2.2 – Potential Energy Diagram

The red arrow in Figure 2.2.2 shows the electronic transition between energy levels. The blue line in Figure 2.2.2 shows the vibrational transition between energy levels. Rotational transitions are transitions within a certain vibrational energy level. Each vibrational transition results in a band in the Raman spectrum of the molecule.

Molecular vibrations can occur as either bending or stretching within the bonds. Specifically, they can either stretch symmetrically or asymmetrically and can either bend in a wagging, twisting, rocking, or scissoring motion. These vibrational modes of a

molecule cause it to remain in constant motion and never sit stationary. A molecule's degree of freedom is 3N, where N is the number of atoms, and this is based off of the three Cartesian coordinates x, y, and z. Molecules have a specific degree of freedom based on it they are linear or non-linear. The normal modes for linear molecules are (3N-5) degrees of freedom and the normal modes for non-linear molecules are (3N-6) degrees of freedom. The vibrational modes and their interactions with radiation give rise to bands in the Raman spectrum.

Chapter 3: Raman Spectroscopy

3.1 Instrumental Design

A Raman spectrometer requires three primary components, a monochromatic light source, a detector, and a sampling device. In the lab conducting this research, the Raman spectrometer consisted of a laser with a specific wavelength as the excitation source (monochromatic light source), a microscope as the sampling device, and a CCD detector, which is a charge coupled device that is described in greater detail later in this chapter. Figure 3.1.1 shows the outline of a typical Raman spectrometer.

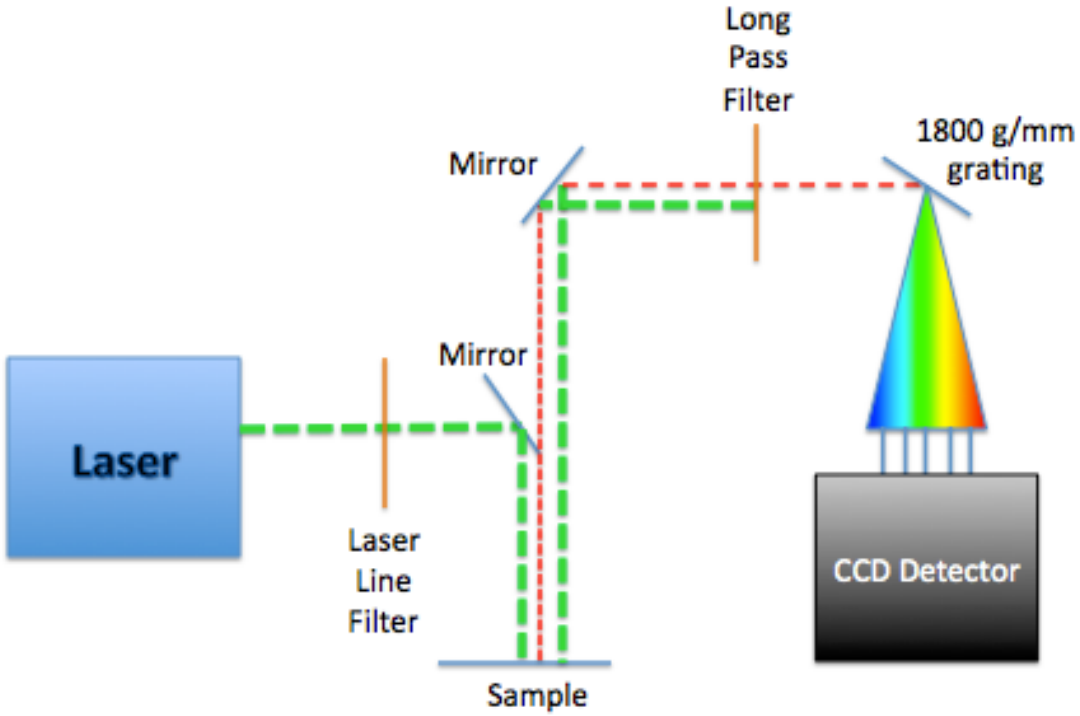

Figure 3.1.1 – Basic instrumental design of a Raman Spectrometer

Usually the lasers used for Raman spectroscopy have wavelengths in the visible light regions; but they range from the ultraviolet region to the infrared region on the

electromagnetic spectrum. The laser is passed through the laser line filter and reflected off of a mirror, projecting the laser onto the sample at a 90 degree angle from the path the incident light. The laser line filter is a filter that only allows the passage of the incident light. The incident light is either absorbed, scattered, or reflected. The scattered and reflected light is projected back towards another mirror that directs the reflected light and the scattered light through a long pass filter. In this research, a 540 long pass filter was used. This filter does not allow light with the same wavelength of the incident light through. This process ensures that the spectrometer is only detecting the light that is inelastically scattered. The scattered light is redirected by mirrors to a monochromator, which uses grating to diffract the beam into a narrow band of wavelengths.[24] The band of wavelengths is measured by the CCD. The charge coupled device is a silicon based multichannel array detector of UV, visible and near- infra light.[25] They are able to turn the current created by the photons hitting the silicon surface into an electrical current able to be read by the spectrometer.

3.2 Raman Spectroscopy Principles

When a monochromatic light, such as a laser, hits the sample, the light is either absorbed or scatted, and this light can scatter at different capacities. Raman spectroscopy is a type of vibrational spectroscopy that measures the inelastic scattering of the monochromatic light that hits the sample and causes electrons to change energy levels. Inelastic scattering occurs when the energy of the incident light is different than the energy of the scattered light. This is what is commonly referred to as the Raman effect.

This fraction is very small; most of the scattered light is elastic and possesses the same energy, frequency, and wavelength as it did before it hit the sample.[18] Elastic scattering is commonly referred to as Rayleigh scattering. Rayleigh scattering occurs when the incident light is not affected by the sample, and the energy of the photon after interacting with the molecule is the same as the energy of the incident photon. In Raman inelastic scattering, the light interacts with the molecule and distorts (polarizes) the cloud of electrons round the nuclei to form a short-lived state called a 'virtual state'. [18] Raman spectrometers can only detect vibrational modes when there is a change in polarizability within the molecule. In order for the Raman effect to occur, there must be a change in dipole moment within the molecule during a normal vibration.[23] In accordance with the Raman selection rule, the molecular polarizability changes as the molecular vibrations displace the constituent atoms from their equilibrium positions.[26] The bigger the change in the molecule's polarizability, the more intense the Raman scattering effect is.

Stokes and anti-Stokes scattering are two variations of the Raman effect. Stokes scattering is when an electron is excited to a higher energy state and then relaxes down to an energy state that is higher than the original energy level. Anti-stokes scattering is just the opposite. An anti-stokes scattering line occurs when a molecule in an excited level rises to a higher, unstable level by interacting with an incident photon and then returns to the ground state upon scattering a photon.[23] In both Stokes scattering and anti-Stokes scattering, the energy of the Raman photon is the difference between the energy of the incident photon and the energy absorbed by the molecule. The photon released after inelastic scattering is commonly referred to as the Raman photon.[27] Figure 3.2.1 illustrates elastic scattering and inelastic scattering.

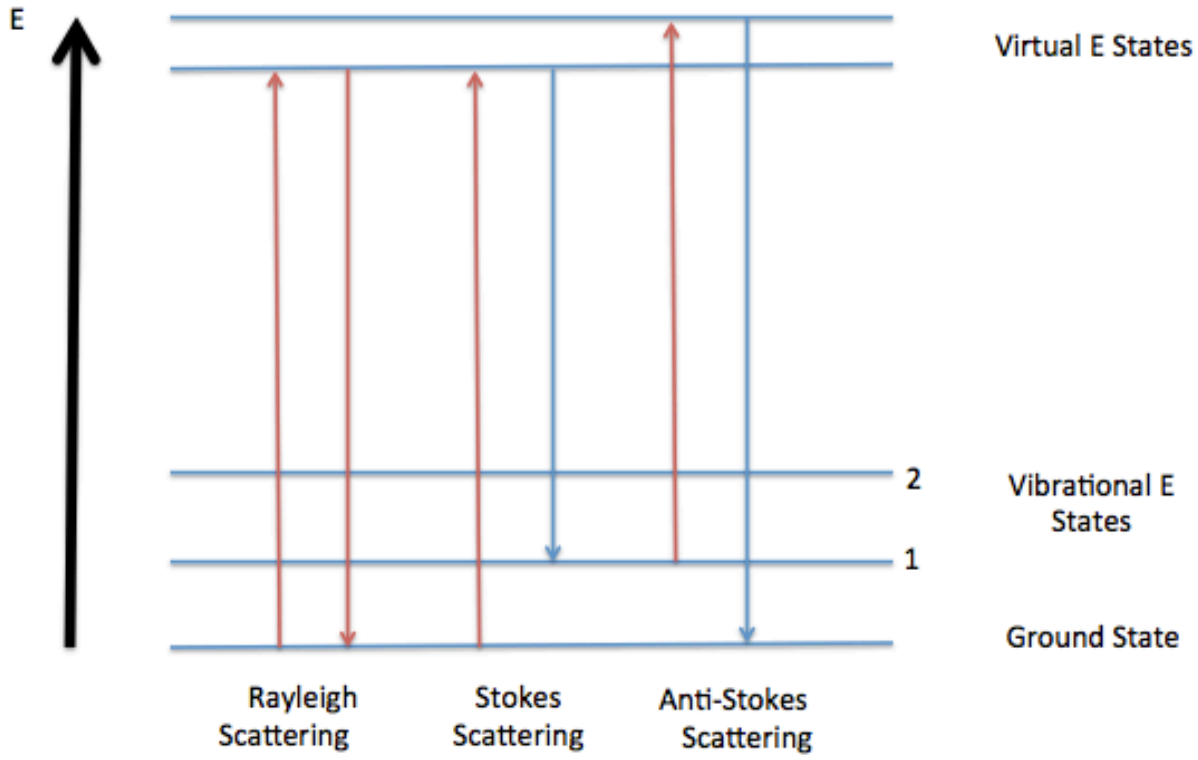

Figure 3.2.1 – Elastic and Inelastic Scattering Diagram

Raman spectroscopy can be used as a fingerprint tool for the sample, providing both quantitative and qualitative measurement information; Raman spectroscopy was utilized in the research required to conduct this thesis.[28] Because different functional groups have different characteristic vibrational energies, every molecule has a unique Raman spectrum.[26]

Raman spectroscopy was used in this research project to collect data on the PLA-PAMAM sample, as well as the PAMAM-boc sample, and compare the way the spectra fluctuates when the sample is in water and when the sample is in a solution with an

unusual pH. pH is a quantitative scale from 0 to 14 referring to the acidity or basicity of a solution. The pH value of a given solution is a measure of the acidity of the hydrogen ion (a_{H^+}) in that solution, as shown in the equation below,[29]

$$pH = -\log [H^+]$$

where $[H^+]$ is the concentration of the hydrogen or hydronium ion. A more acidic solution will have a lower pH and a more basic solution will have a higher pH. Because the scale is logarithmic, the hydrogen or hydronium ion activity is 10 times greater at a pH of 3 than a pH of 4.[29] Because this biomaterial is being studied as a drug delivery system, it is important to study a range of pH's that occurs in the human body. For example, the eye is more basic than water so the effects of a higher pH on the structure is extremely beneficial.[29]

As stated above, Raman spectroscopy is a vibrational method of spectroscopy that detects the shift in energy of scattered light. A laser is shined on the sample and the light is scattered. The Raman shift shown in the spectrum is the difference in energy between the incident photon and the scattered photons. Different functional groups of molecules can be analyzed from a Raman spectrum because of the unique changes in energy between the incident photons and the scattered photons from the different vibrational bonds. Different bonds give different signals on the Raman spectrometer, and this allows for Raman spectra to be a resourceful footprinting tool for identifying characteristics of molecules. Strong bonds between lightly weighted atoms have a high Raman shift and the heavier atoms with weaker bonds have a lower Raman shift. For example, a carbon carbon double bond occurs around the 1600 cm^{-1} mark on a Raman graph, compared to 800 cm^{-1} for a single bond between two carbon atoms.

3.3 Computational Methods

The computational results of PAMAM-boc and PLA-PAMAM were produced in order to compare the theoretical results to the experimental results and explain the findings. The theoretical results and the computational methods that lead to the results are based on quantum mechanics and the time independent Schrödinger equation. The time independent Schrödinger equation is a wave equation that predicts the future behavior of a system with a wave-particle nature. This equation is shown below:

$$\hat{H}\psi_n = E\psi_n$$

In the Schrödinger equation above, the H stands for the Hamiltonian factor, which is the total energy operator and describes the potential energy and the kinetic energy of the particles of the system. E is the total energy of the system and ψ_n is the wavefunction that describes the three-dimensional state of the system with the principle quantum number, n.[30]

Gaussian 09 is the software program that is used in computational chemistry. Because the time independent Schrödinger equation only works perfectly for one electron systems, *Gaussian 09* is used to approximate the solutions of the time independent Schrödinger equation for multiple electron systems. While the theoretical calculations are inaccurate because assumptions must be made for multi-electron systems, they provide a good comparison to the experimental results. The calculations of the Schrödinger equation search the potential energy surface for a single point in the energy value. The program optimizes the different geometrical configurations of the structure and places it in the conformation with the lowest energy. The B3LYP method and the 6-311++G(*d*,*p*) basis set were used in the computational study of the structure. B3LYP is a

hybrid method of the density functional theory, which is a computational method that utilizes the electron density of a molecule to provide molecular characteristics and properties. A basis set is a set of functions that builds molecular orbitals by turning partial differential equations into functional algebraic equations by representing the electronic wave function. The larger the basis set, the more functions included and the more accurate the molecular orbital representations. By using the keyword "Freq=Raman" and instructing *Gaussian 09* to compute the force constants and to produce vibrational frequencies, the computational spectra can be compared to the experimental data to explain shifts upon hydration.

Chapter 4: Raman Spectroscopic Analysis of PLA-PAMAM

4.1 Experimental Results and Data Analysis

Raman data was taken of PAMAM-boc, which is the hydrophilic portion of the LDBC, PLA-PAMAM. This data preceded the Raman analysis of PLA-PAMAM to understand the way this one portion of the molecule changes in response to the environment. The results are then compared to the Raman data for the entire amphipathic polymer. Dr. Watkins supplied the crystalline samples of PAMAM-boc and PLA-PAMAM. Table 4.1.1 lists the stretches for common functional groups at their respective wavelengths.

Bond Type	Expected Frequency Range of Peak
O-H	3200-3700
N-H	3300-3500
C-O	1050-1150
C=O	1670-1820
C-H	2850-3100
C=C	1620-1680
C≡C	2100-2260
C-N	1250-1335
C=N	2100-2270
C≡N	2210-2260
S-C	570-710
S=C	1030-1200

Table 4.1.1 – Common Vibrational Frequencies

Figure 4.1.1 compares the full spectrum from 0 cm^{-1} to 4000 cm^{-1} for PAMAM-boc alone and PAMAM-boc surrounded by a drop of pure water. This spectrum is important for the analysis of the PAMAM-boc structure while it's interacting with water. If this biomaterial is to be used as an effective drug delivery system, it must be able to interact in water. The analysis of the dendrimer portion of the LDBC alone will aid in the analysis of the entire amphipathic structure, which is discussed later in this thesis. The important stretches of Raman are the stretches including the atoms carbon, hydrogen, oxygen, and nitrogen. PLA-PAMAM is comprised of these atoms and shifts involving these atoms are important for this research and thesis.

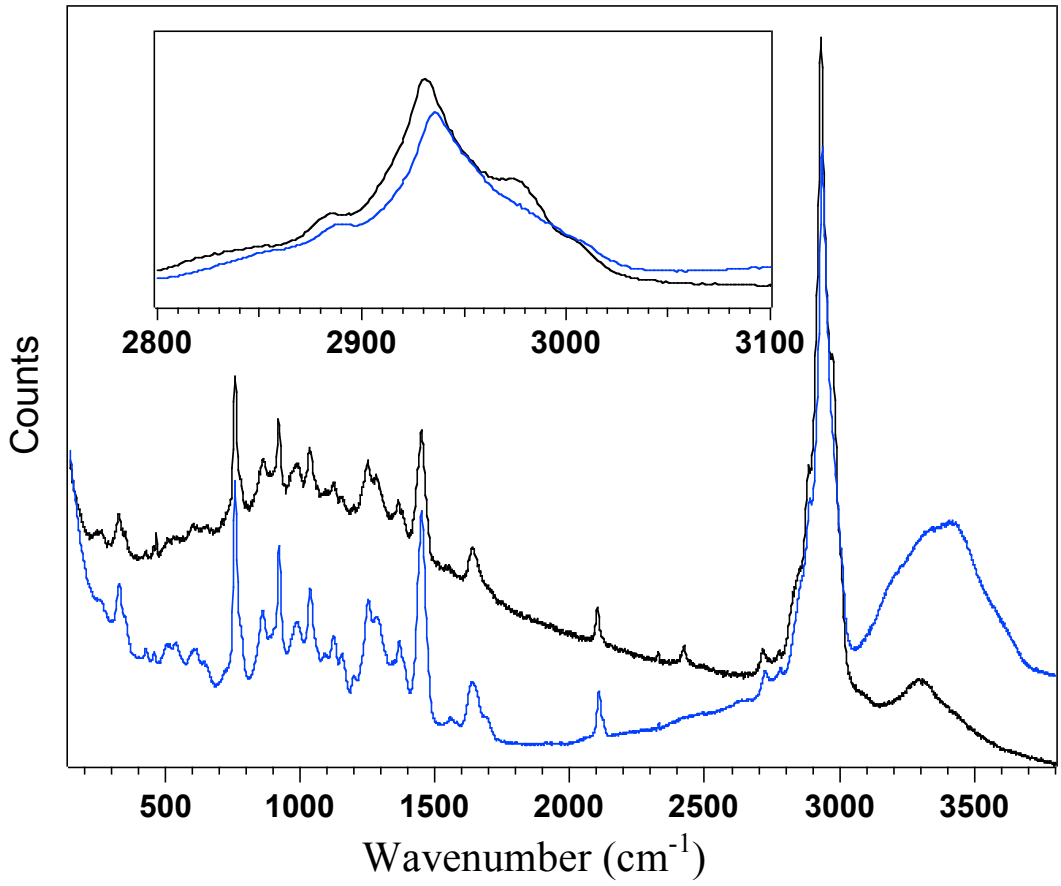

Figure 4.1.1 – Comparative Raman spectra of PAMAM-boc (black) and PAMAM-boc in water (blue).

The black line represents the PAMAM-boc spectrum alone, without water. The blue line represents the PAMAM-boc spectrum interacting with water. The spectra are compared by looking at any specific shifts in the peaks and analyzing what the cause could be that gives rise to the shifts. The only notable difference in the two spectra is seen around 3000 cm^{-1}, which will be discussed later in this chapter.

Figure 4.1.2 is the low energy spectra of PAMAM-boc and PAMAM-boc surrounded by water. The spectrum is beneficial because it allows for a closer analysis of the spectrum and any shifts that may have occurred can be visualized easier.

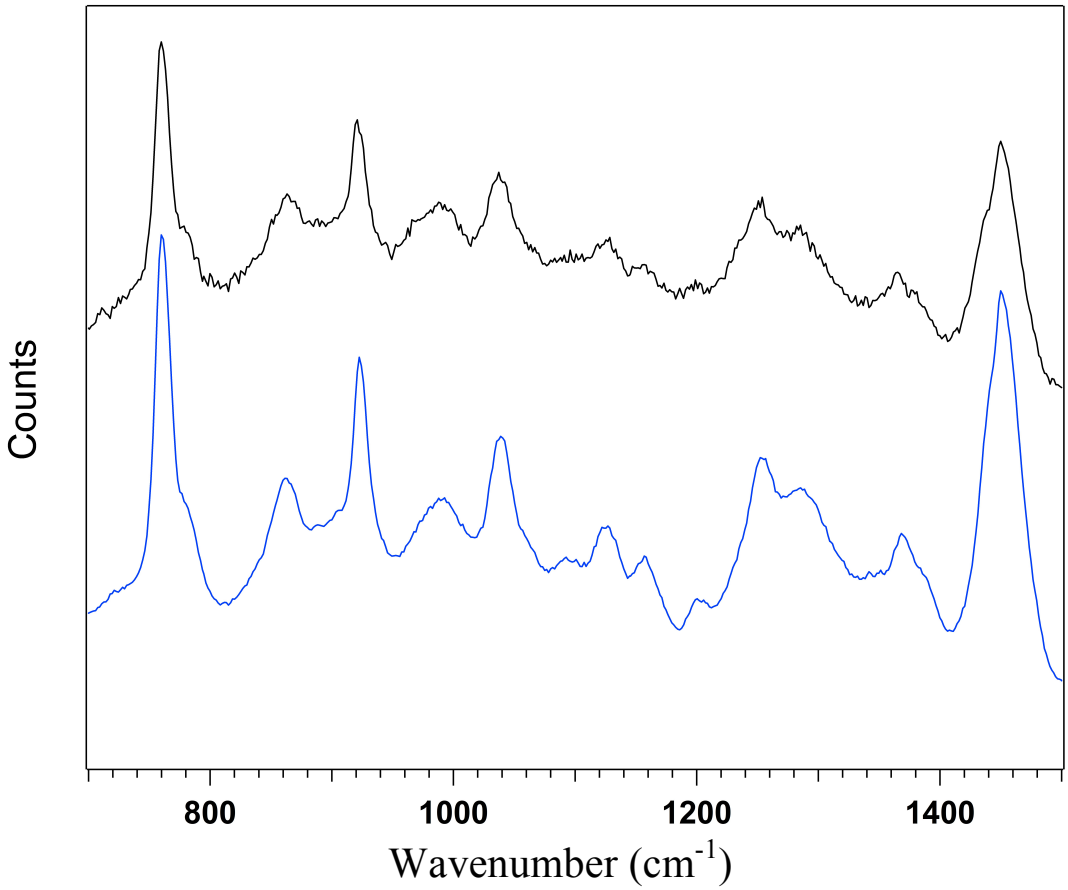

Figure 4.1.2 – Low energy spectra of PAMAM-boc (black) and PAMAM-boc in water (blue).

The low energy end of the Figure 4.1.2 entire spectrum is above and shifts are minimal to none. There are no noticeable shifts in the large peaks occurring at the 760 cm^{-1} mark and the 1450 cm^{-1} mark. There are also no notable shifts in the smaller peaks around the 940 cm^{-1}, 1040 cm^{-1}, and 1260 cm^{-1} marks. There were no shifts in the peaks, meaning the sample being studied under the Raman spectrometer did not alter its structure, or more specifically its vibrational modes or bond vibrations, so the Raman activity is the same for PAMAM-boc alone and PAMAM-boc surrounded by a drop of water. The important stretches occurring in this region of the Raman spectrum that are of relevance to this thesis are the C-C stretches, the C-N stretches, and the C-O stretches. Hydrogen bonding between the hydrogen in the water molecules and the oxygen and nitrogen in the PAMAM-boc sample was expected, but the results do not show any changes in the structure that imply any such bonding happened.

Figure 4.1.3 shows the high energy end of the spectrum depicted in Figure 4.1.1. The C-H stretching region occurs between 2800 cm^{-1} and 3300 cm^{-1}. This region of the spectrum was expected to not have any shifts in peaks because the hydrophobic C-H bonds should not affect the neutral PAMAM-boc. However, there was a slight shift around the 3000 cm^{-1} mark. The reason for this could be that the hydrophilic portion of the molecule is making the water form an ordered structured shell around it or this could be due to perturbations to N-H stretches.

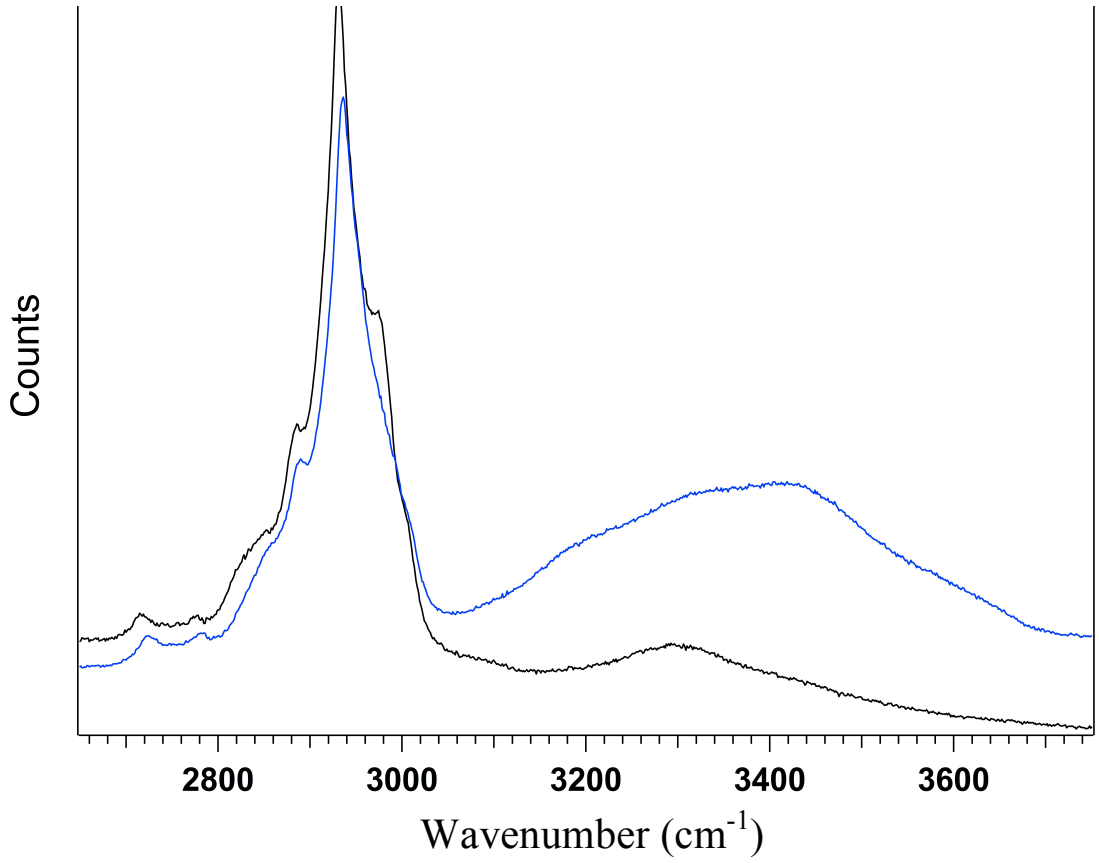

Figure 4.1.3 – High energy spectra of PAMAM-boc (black) and PAMAM-boc in water (blue).

Figure 4.1.4 shows a full spectrum, comparing the whole PLA-PAMAM structure with the PLA-PAMAM structure surrounded by a droplet of water. The Raman data was taken for both samples and Figure 4.1.5 allows for the two spectra to be compared next to each other. Figure 4.1.5 and Figure 4.1.6 are the low energy spectrum of Figure 4.1.4 and the high energy spectrum of Figure 4.1.4, respectively. These two figures allow for a more precise analysis of the two spectra and the comparison is much easier to see when the graphs are narrowing in more on one specific area of the overall Raman spectrum of PLA-PAMAM.

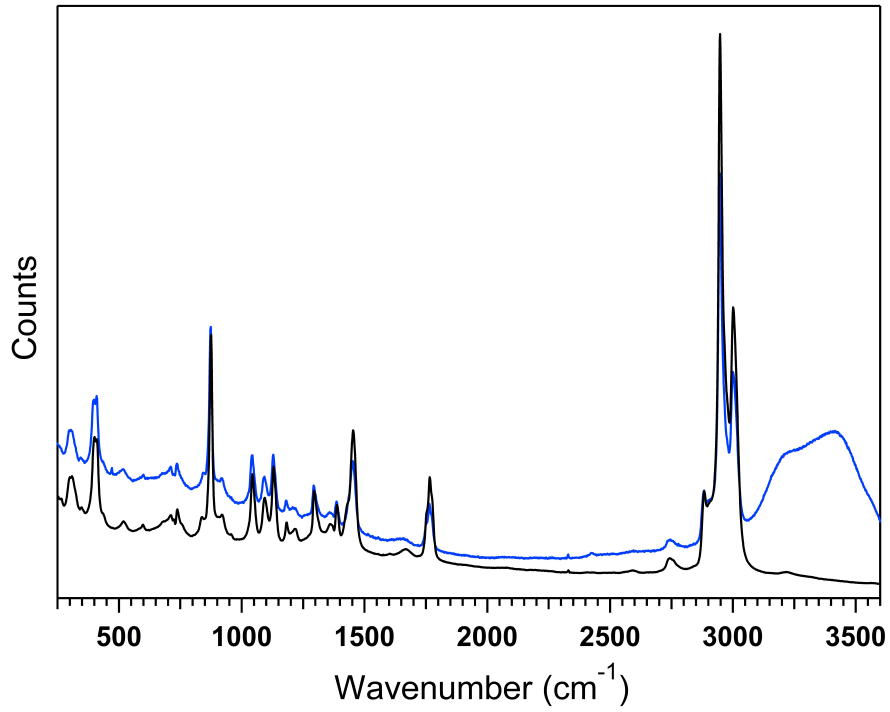

Figure 4.1.4 – Comparative Raman spectra of PLA-PAMAM (black) and PLA-PAMAM in water (blue).

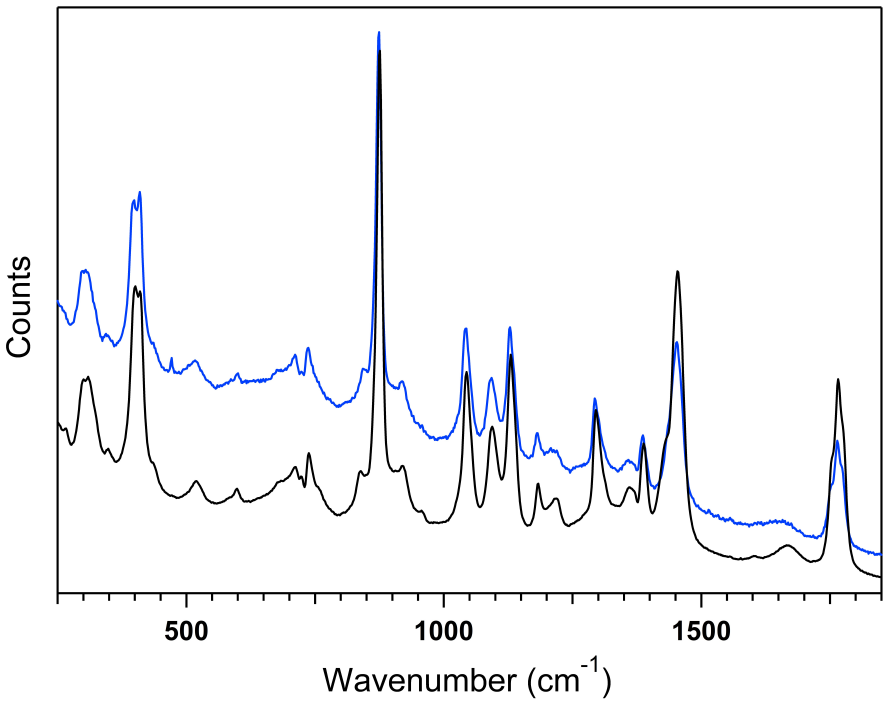

Figure 4.1.5 – Low energy spectra of PLA-PAMAM (black) and PLA-PAMAM in water (blue).

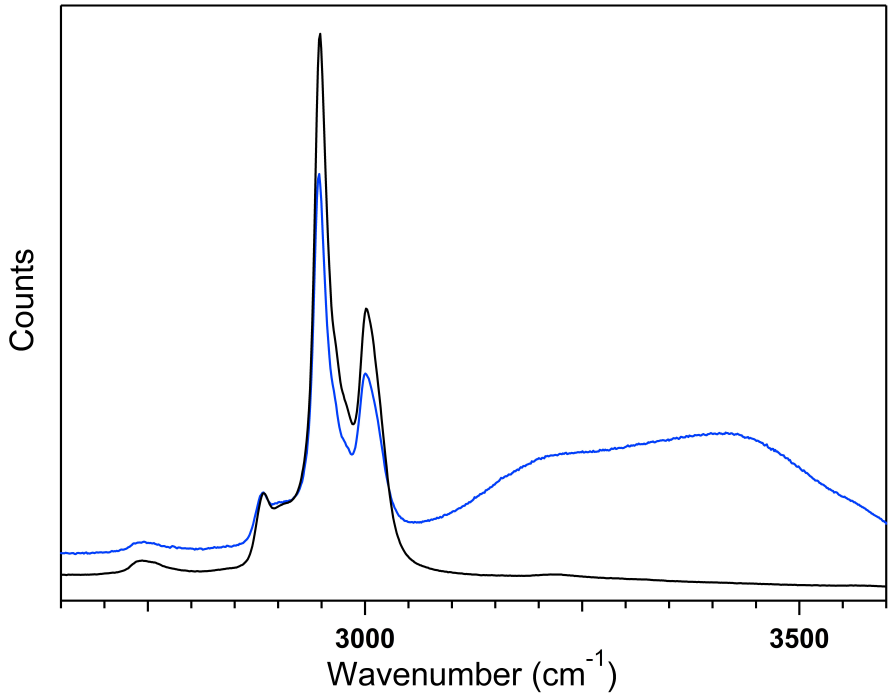

Figure 4.1.6 – High energy spectra of PLA-PAMAM (black) and PLA-PAMAM in water (blue).

The full spectrum, the low energy spectrum, and the high energy spectrum of PLA-PAMAM do not show any significant shifts at any peaks. There were expecting to be shifts as the hydrophilic portion of the LDBC, PAMAM, interacted with the water droplet. However, no such interactions occurred, as the spectra show no shifts in peaks at any point.

Figure 4.1.7 compares the Raman spectra of PLA-PAMAM as aggregates in water to the Raman spectra PLA-PAMAM as aggregates in a pH buffer solution of 9.6. The pH buffer solution was made by mixing Sodium Bicarbonate with water and adding sufficient amount of Hydrochloric Acid and Sodium Hydroxide to the solution to change the pH. The pH of the buffer solution was 9.6, which is a basic solution. A 1 mL

sample was prepared consisting of 0.5 mL of the buffer solution and 0.5 mL of the aggregated PLA-PAMAM in water.

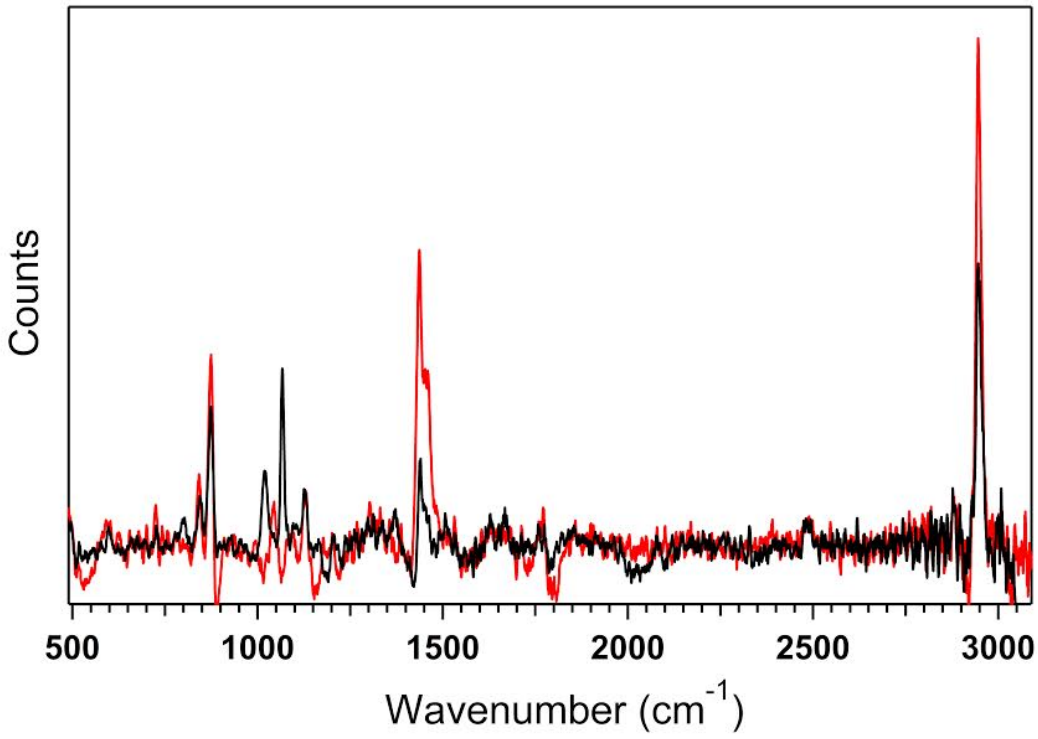

Figure 4.1.7 – Comparative spectra of PLA-PAMAM aggregate in water (black) and PLA-PAMAM in a 9.6 pH buffer solution (red)

The Raman spectrum was taken and is shown as the black line in Figure 4.1.7. Shifts in the spectra occur around 1200 cm^{-1}. These shifts are minimal, but could have occurred as the result of a number of hydrogen atoms being taken off by the basic environment of a pH 9.6 solution, leading to the degradation of the material. The shifts could also have resulted from a difference in the water networking that surrounded the aggregates. If the pH caused the water networking system to change, the bending and stretching of the bonds could have been different in that solution.

4.2 Theoretical Results and Data Analysis

The theoretical results for this thesis are produced in order to explain the experimental results. The figures below are two optimized images that were produced using the program *Gaussian 09*. They are optimized in *Gaussian 09* to produce the structural conformation with the lowest energy. These images are helpful because they provide the different stretches and bends that explain the shifts in the experimental data spectra.

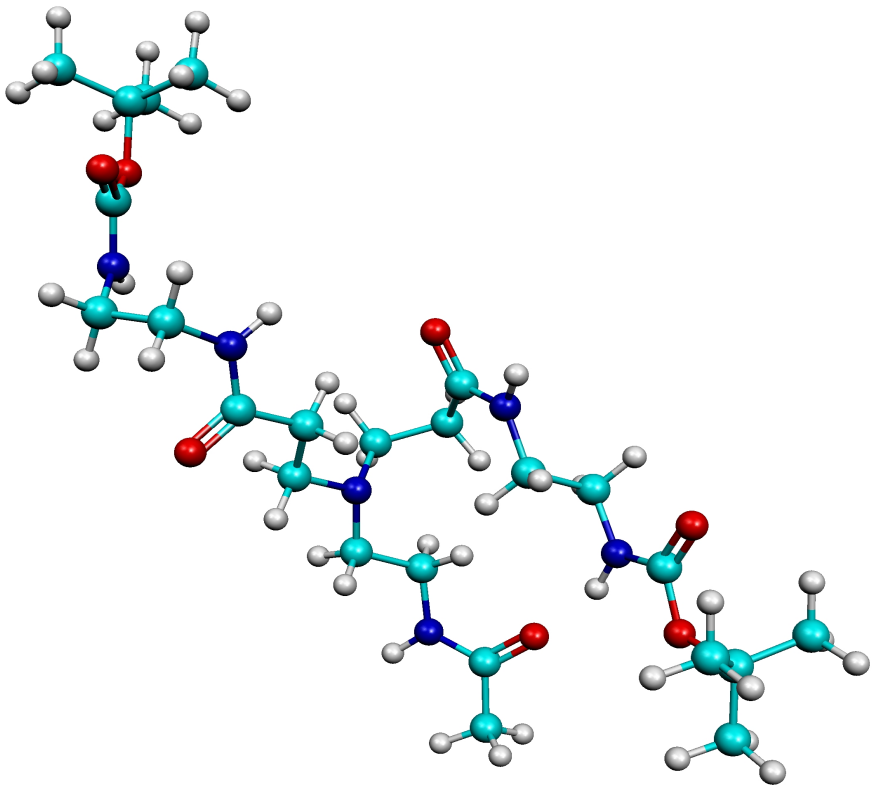

Figure 4.2.1 – Optimized structure of PAMAM-boc with higher energy

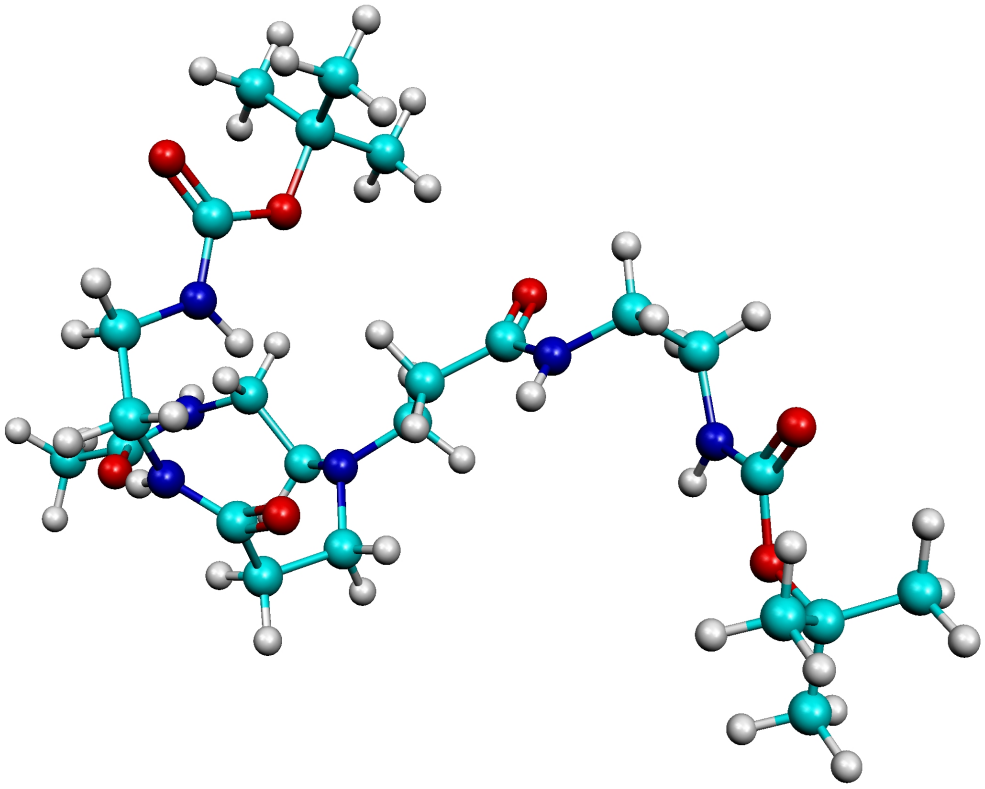

Figure 4.2.2 – Optimized structure of PAMAM-boc with lower energy

Using the optimized structure of PAMAM-boc with low energy, the changes in figure 4.1.4 were analyzed. There was a missing bulge from the curve around 3000 cm^{-1}. After using *Gaussian 09* and the optimized PAMAM-boc structure, it was found that the bulge was less intense. The activity around this frequency is C-H bending and stretching, and the surrounding water molecules forming a network around the PAMAM-boc could explain the decrease in intensity.

Figures 4.2.3 and 4.2.4 show the theoretical Raman spectra of the optimized structures of PAMAM-boc in different energy regions. The bottom spectrum is the

experimental results from the PAMAM-boc. The middle spectrum is the theoretical yield of the computational optimized PAMAM-boc with higher energy. The top spectrum is the theoretical yield of the computational optimized PAMAM-boc with lower energy, which is the optimized structure used in this thesis to compare theoretical results to experimental results. The two theory spectra were scaled by 0.965 to line up with the experimental spectra. Thus, the two spectra could be looked at under close comparison and the differences between the three spectra were easier to visualize.

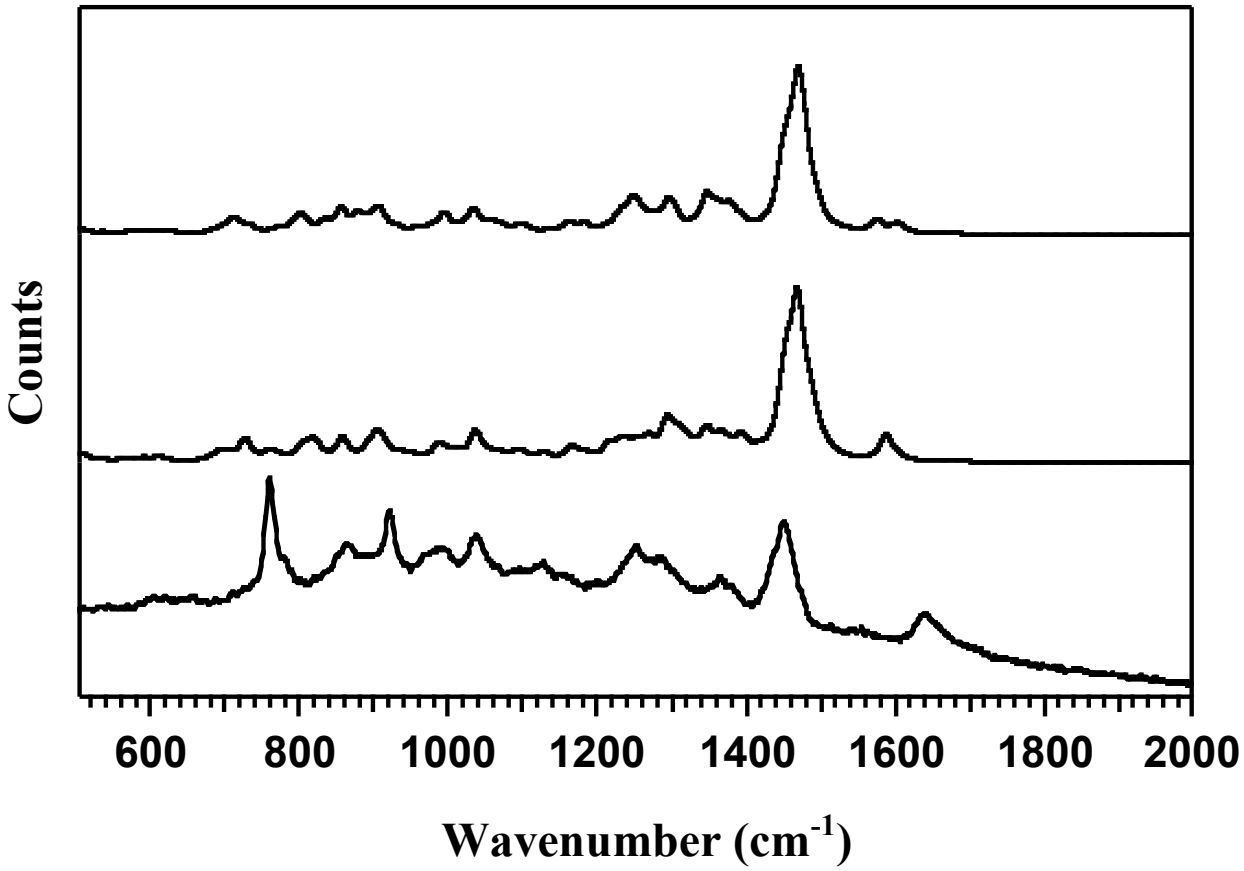

Figure 4.2.3 – Comparative spectra of theoretical (top: low energy and middle: high energy structures) and experimental (botrtom) Raman spectra of PAMAM-boc at low energy

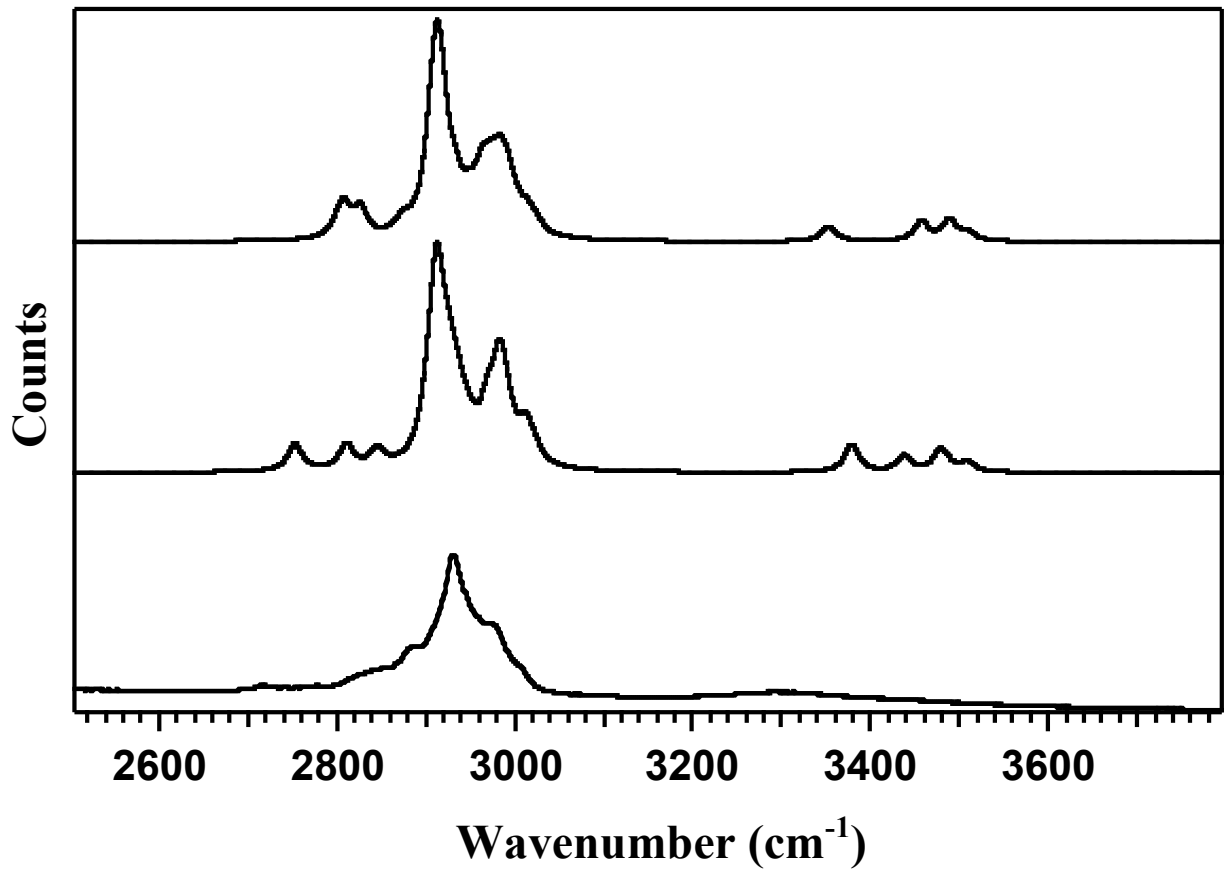

Figure 4.2.4 - Comparative spectra of theoretical (top: low energy and middle: high energy structures) and experimental (botrtom) Raman spectra of PAMAM-boc at high energy

Calculations involving water hydrogen bonded to N-H groups are currently underway to see if these interactions can account for the shifts observed with PAMAM-boc.

4.3 Discussion and Conclusions

The results from the Raman spectrometer and the computational results allow for

the analysis of PAMAM-boc and PLA-PAMAM and the way the environment affects their behavior. The linear dendritic block copolymer, PLA-PAMAM, aggregates in water, forming beneficial vesicle-like structures that are being studied for their drug delivery system capabilities. Their branched structure with controlled terminal groups allows for the encasing of drugs within the pockets of the branches. Because of the quick spike and sudden drop off of drug effects in the body, PLA-PAMAM offers a route to continuously release a steady amount of drugs when the body is in need and stimulates the LDBC to release its contents. PLA-PAMAM responding to different stimuli, temperature or pH for example, allows the body to replenish itself with drugs when it stimulates the LDBC. This thesis explores the effects of hydrogen bonding by water and pH on PAMAM-boc and PLA-PAMAM. One potential entry for PLA-PAMAM into the body is through the eye, which has a basic pH above 7. Comparing Raman data of PLA-PAMAM and PAMAM-boc alone, in water, and in a basic pH solution illustrates the structural changes by utilizing Raman spectroscopy and computational methods.

This research shows that PAMAM-boc's structure was not drastically changed when placed in a droplet of water. The only noticeable difference in the spectra was the disappearance of a portion of a peak around 3000 cm^{-1}. This disappearance could've been caused by the ordered structured shell of water because of the influence of the hydrophilic portion of PAMAM-boc. This hypothesis was made possible through the use of *Gaussian 09* and computational chemistry. The differences in structure of PLA-PAMAM alone and in water are inferred to very minimal from the experimental. There were no shifts in spectral peaks between PLA-PAMAM and PLA-PAMAM surrounded by a droplet of water. It was expected to see a shift in the hydrophilic portion of

PAMAM as it interacted with water; however, no such interactions were illustrated in the spectra. Comparing the aggregated PLA-PAMAM vesicles in water to the aggregated PLA-PAMAM vesicles in a pH buffer solution of 9.6, there was a slight shift in peaks around 1200 cm^{-1}. This change could have occurred as the result of a number of hydrogen atoms being taken off by the basic environment of a pH 9.6 solution. Calculations involving water hydrogen bonded to N-H groups are currently underway to see if these interactions can account for the shifts observed with PAMAM-boc.

This thesis made it possible to examine the structural differences of PAMAM-boc, as well as PLA-PAMAM when they are placed in different environments. Surprisingly, the structural changes were overall minimal. This research will provide basic foundational information for further research conducted using PAMAM-boc and PLA-PAMAM. The study and analysis of this linear dendritic block copolymer is important for the scientific community, and PLA-PAMAM as an effective drug delivery system will be a huge achievement in biomedical applications.

References

1. Overview of Biomaterials and Their use in Medicinal Devices. ASM International. 1-11.
2. Yoshida, R.; Okano, T., Stimuli-Responsive Hydrogels and Their Application to Functional Materials. **2010**, 19-43.
3. Priya James, H.; John, R.; Alex, A.; Anoop, K. R., Smart polymers for the controlled delivery of drugs - a concise overview. *Acta Pharm Sin B* **2014,** *4* (2), 120-7.
4. Han, L. H.; Lai, J. H.; Yu, S.; Yang, F., Dynamic tissue engineering scaffolds with stimuli-responsive macroporosity formation. *Biomaterials* **2013,** *34* (17), 4251-8.
5. Sen, C. K., Wound healing essentials: let there be oxygen. *Wound Repair Regen* **2009,** *17* (1), 1-18.
6. You, J. O.; Rafat, M.; Almeda, D.; Maldonado, N.; Guo, P.; Nabzdyk, C. S.; Chun, M.; LoGerfo, F. W.; Hutchinson, J. W.; Pradhan-Nabzdyk, L. K.; Auguste, D. T., pH-responsive scaffolds generate a pro-healing response. *Biomaterials* **2015,** *57*, 22-32.
7. Hsu, H. J.; Bugno, J.; Lee, S. R.; Hong, S., Dendrimer-based nanocarriers: a versatile platform for drug delivery. *Wiley Interdiscip Rev Nanomed Nanobiotechnol* **2017,** *9* (1).
8. Madaan, K.; Kumar, S.; Poonia, N.; Lather, V.; Pandita, D., Dendrimers in drug delivery and targeting: Drug-dendrimer interactions and toxicity issues. *J Pharm Bioallied Sci* **2014,** *6* (3), 139-50.
9. Caminade, A.-M.; Turrin, C.-O., Dendrimers for drug delivery. *Journal of Materials Chemistry B* **2014,** *2* (26), 4055-4066.
10. Caminade, A. M.; Laurent, R.; Zablocka, M.; Majoral, J. P., Organophosphorus chemistry for the synthesis of dendrimers. *Molecules* **2012,** *17* (11), 13605-21.
11. Fox, M. E.; Szoka, F. C.; Frechet, J. M., Soluble polymer carriers for the treatment of cancer: the importance of molecular architecture. *Acc Chem Res* **2009,** *42* (8), 1141-51.
12. (a) Kesharwani, P.; Banerjee, S.; Gupta, U.; Mohd Amin, M. C. I.; Padhye, S.; Sarkar, F. H.; Iyer, A. K., PAMAM dendrimers as promising nanocarriers for RNAi therapeutics. *Materials Today* **2015,** *18* (10), 565-572; (b) Jonathan D. Eichman, A. U. B., Jolanta F. Kukowska-Latallo, James R. Baker Jr. , <The use of PAMAM dendrimers in the efficient transfer of genetic material into cells.pdf>.
13. Pearson, R. Dendritic Nanoparticles: The next generation of nanocarriers? 1-51.
14. Wurm, F.; Frey, H., Linear–dendritic block copolymers: The state of the art and exciting perspectives. *Progress in Polymer Science* **2011,** *36* (1), 1-52.
15. Vandenabeele, P., Raman spectroscopy. *Anal Bioanal Chem* **2010,** *397* (7), 2629-30.
16. Electromagnetic Theory & Maxwell's Equations. Chapter 1. 1-33.
17. Sathyanarayana, D. N., *Vibrational Spectroscopy: Theory and Applications*. New Age International (P) Limited: 2015.
18. Smith, E. Modern Raman Spectroscopy - A Practival Approach. Wiley. 2005.
19. Paschotta, R., Field Guide to Lasers. *SPIE Press* **2008**.
20. Hilborn, R. C., Einstein coefficeients, cross sections, f values, dipole moments, and all that *Department of Physics, Oberline College* **1981**.
21. Engel, T., Reid, Phillip, , Physical Chemistry. *Pearson Education* **2013,** *Vol. 3*.

22. Steele, D., Theory of Vibrational Spectroscopy. *W.B. Saunders Company* **1971,** *Volume 8*.
23. Freeman, S. K., *Applications of Laser Raman Spectroscopy*. John Wiley & Sons Inc. : Union Beach, New Jersey, 1974.
24. Raman Spectroscopy. Gamry Instruments. https://www.gamry.com/application-notes/EIS/raman-spectroscopy/.
25. What is a CCD detector? Horriba Scientific. http://www.horiba.com/scientific/products/raman-spectroscopy/raman-academy/raman-faqs/what-is-a-ccd-detector/.
26. Haynes, C. L., Surface Enhanced Raman Spectroscopy.
27. Rulli, C. Raman Spectroscopy. https://www.sas.upenn.edu/~crulli/RamanBasics.html.
28. Chang, C.-C.; Chiu, Y., Applying quantitative micro-Raman spectroscopy to analyze stone compositions extracted from ureteroscopic lithotripsy urine. *Urological Science* **2016**.
29. Lawn, R.; Prichard, E., *Measurement of PH*. Royal Society of Chemistry: 2003.
30. Tro, N. J., *Chemistry : a molecular approach*. 2014.